HHS Public Access

Author manuscript

Crit Care Med. Author manuscript; available in PMC 2017 September 01.

Published in final edited form as:

Crit Care Med. 2016 September ; 44(9): e854–e865. doi:10.1097/CCM.0000000000001721.

Comparative Effects of Volutrauma and Atelectrauma on Lung Inflammation in Experimental Acute Respiratory Distress Syndrome

Andreas Güldner, MD[1], **Anja Braune, MSc**[1], **Lorenzo Ball, MD**[1,2], **Pedro L. Silva, PhD**[1,3], **Cynthia Samary, MSc**[1,3], **Angelo Insorsi, MD**[1,2], **Robert Huhle, MSc**[1], **Ines Rentzsch, PhD**[1], **Claudia Becker**[1], **Liane Oehme, PhD**[4], **Michael Andreeff, PhD**[4], **Marcos F. Vidal Melo, MD, PhD**[5], **Tilo Winkler, PhD**[5], **Paolo Pelosi, MD, FERS**[2], **Patricia R. M. Rocco, MD, PhD**[2], **Jörg Kotzerke, MD, PhD**[4], and **Marcelo Gama de Abreu, MD, MSc, PhD, DESA**[1]

[1]Department of Anesthesiology and Intensive Care Medicine, Pulmonary Engineering Group, University Hospital Dresden, Technische Universität Dresden, Dresden, Germany

[2]IRCCS San Martino IST, Department of Surgical Sciences and Integrated Diagnostics, University of Genoa, Genoa, Italy

[3]Laboratory of Pulmonary Investigation, Carlos Chagas Filho Biophysics Institute, Federal University of Rio de Janeiro, Rio de Janeiro, Brazil

[4]Institute of Nuclear Medicine, University Hospital Dresden, Dresden, Germany

[5]Department of Anesthesia, Critical Care and Pain Medicine, Massachusetts General Hospital, Harvard University, Boston, MA

Abstract

Objective—Volutrauma and atelectrauma promote ventilator-induced lung injury, but their relative contribution to inflammation in ventilator-induced lung injury is not well established. The aim of this study was to determine the impact of volutrauma and atelectrauma on the distribution of lung inflammation in experimental acute respiratory distress syndrome.

Address requests for reprints to: Dr. Marcelo Gama de Abreu, MD, MSc, PhD, DESA, Department of Anesthesiology and Intensive Care Medicine, Pulmonary Engineering Group, University Hospital Carl Gustav Carus, Technische Universität Dresden, Fetscherstr. 74, 01307 Dresden, Germany. mgabreu@uniklinikum-dresden.de.

Supplemental digital content is available for this article. Direct URL citations appear in the printed text and are provided in the HTML and PDF versions of this article on the journal's website (http://journals.lww.com/ccmjournal).

This work was performed by the Pulmonary Engineering Group, Department of Anesthesiology and Intensive Care Medicine, and the Institute of Nuclear Medicine, University Hospital Carl Gustav Carus, Technische Universität Dresden, Dresden, Germany.

Ms. Braune disclosed work for hire. Mr. Huhle disclosed work for hire. Dr. Vidal Melo received support for article research from the National Institutes of Health (NIH). His institution received grant support from RO1 HL 121228, NIH, and Merck (current investigator-initiated grant from Merck). Dr. Kotzerke's institution received grant support from Deutsche Forschungsgemeinschaft. Dr. Gama de Abreu served as a board member for Ventinova EV (Eindhoven, The Netherlands); consulted for Dräger Medical AG (Lübeck, Germany) and Novalung GmbH (Heilbronn, Germany); lectured for Dräger Medical AG (Lübeck, Germany), Novalung GmbH (Heilbronn, Germany), and GE Healthcare (Paris, France); received support for the development of educational presentations from Dräger Medical AG (Lübeck, Germany); received support for travel from Dräger Medical AG (Lübeck, Germany), Novalung GmbH (Heilbronn, Germany), and GE Healthcare (Paris, France); and received support for article preparation from Dräger Medical AG (Lübeck, Germany). His institution received grant support from the German Research Foundation (Governmental Institution; research grant). The remaining authors have disclosed that they do not have any potential conflicts of interest.

Design—Laboratory investigation.

Setting—University-hospital research facility.

Subjects—Ten pigs (five per group; 34.7–49.9 kg)

Interventions—Animals were anesthetized and intubated, and saline lung lavage was performed. Lungs were separated with a double-lumen tube. Following lung recruitment and decremental positive end-expiratory pressure trial, animals were randomly assigned to 4 hours of ventilation of the left (ventilator-induced lung injury) lung with tidal volume of approximately 3 mL/kg and 1) high positive end-expiratory pressure set above the level where dynamic compliance increased more than 5% during positive end-expiratory pressure trial (volutrauma); or 2) low positive end-expiratory pressure to achieve driving pressure comparable with volutrauma (atelectrauma). The right (control) lung was kept on continuous positive airway pressure of 20 cm H_2O, and Co_2 was partially removed extracorporeally.

Measurements and Main Results—Regional lung aeration, specific [^{18}F]fluorodeoxyglucose uptake rate, and perfusion were assessed using computed and positron emission tomography. Volutrauma yielded higher [^{18}F]fluorodeoxyglucose uptake rate in the ventilated lung compared with atelectrauma (median [interquartile range], 0.017 [0.014–0.025] vs 0.013 min^{-1} [0.010–0.014min^{-1}]; $p < 0.01$), mainly in central lung regions. Volutrauma yielded higher [^{18}F]fluorodeoxyglucose uptake rate in ventilator-induced lung injury versus control lung (0.017 [0.014–0.025] vs 0.011 min^{-1} [0.010–0.016min^{-1}]; $p < 0.05$), whereas atelectrauma did not. Volutrauma decreased blood fraction at similar perfusion and increased normally as well as hyperaerated lung compartments and tidal hyperaeration. Atelectrauma yielded higher poorly and nonaerated lung compartments, and tidal recruitment. Driving pressure increased in atelectrauma.

Conclusions—In this model of acute respiratory distress syndrome, volutrauma promoted higher lung inflammation than atelectrauma at comparable low tidal volume and lower driving pressure, suggesting that static stress and strain are major determinants of ventilator-induced lung injury.

Keywords

acute respiratory distress syndrome; atelectrauma; [^{18}F]fluorodeoxyglucose; positron emission tomography; ventilator-induced lung injury; volutrauma

Mechanical ventilation (MV) is frequently required to support the respiratory function and relieve the work of breathing in patients suffering from the acute respiratory distress syndrome (ARDS) (1). However, MV itself has the potential to worsen lung injury (ventilator-induced lung injury [VILI]) (2). MV with low tidal volumes (V_T) has been suggested to minimize damage from tidal over-distension, that is, volutrauma. In addition, positive end-expiratory pressure (PEEP) has been used to stabilize the lung at end-expiration, reducing cyclic closing and reopening of small airways and alveoli, that is, atelectrauma. Both volutrauma and atelectrauma have been proposed as potential mechanisms of VILI (3, 4) and may coexist at different levels of V_T and PEEP despite the use of protective MV in ARDS (5). However, depending on particular settings, as well as the characteristics of lung injury, one of those mechanisms may prevail (6, 7). Therefore,

knowledge of the relative contribution of atelectrauma and volutrauma to VILI can be useful for optimizing protective MV.

VILI is usually accompanied by infiltration and activation of neutrophils in lung tissue (8, 9). Since their activity is mainly supported by anaerobic glycolysis, activated neutrophils have a rate of glucose utilization higher than other inflammatory or lung cells (10, 11). [^{18}F]-fluorodeoxyglucose ([^{18}F]FDG) is a glucose analogue that, after entering cells, does not undergo further metabolism and remains trapped (12). Thus, the uptake rate of [^{18}F]FDG during lung injury is highly correlated with in situ neutrophil activation and inflammation (12).

In the present study, we used lung imaging with CT, PET and tracer kinetic modeling to investigate the impact of atelectrauma and volutrauma on the lung uptake of [^{18}F]FDG in experimental ARDS in pigs. Since static stress and strain, defined as airway pressure and gas volume at PEEP, respectively, are higher in the inflated than collapsed lungs, we hypothesized that volutrauma leads to higher lung inflammation than atelectrauma at comparable low V_T and driving pressure (ΔP), defined as the difference between inspiratory plateau pressure and PEEP.

MATERIALS AND METHODS

Detailed Materials and Methods are presented in the **supplemental data** (Supplemental Digital Content 1, http://links.lww.com/CCM/B808). The Institutional Animal Care and Welfare Committee and the Government of the State of Saxony, Germany, approved all animal procedures, in accordance to federal law.

Preparation

After premedication, 10 pigs (34.7–49.9 kg) were anesthetized, paralyzed, mechanically ventilated in supine position, and continuously monitored for hemodynamics and respiratory system mechanics. Lungs were ventilated in volume-controlled mode using the following settings: fraction of inspired oxygen (FIo_2) of 1.0, V_T of 8 mL/kg, PEEP of 8 cm H_2O, inspiratory:expiratory (I:E) ratio of 1:1, airway flow of 35 L/min, and respiratory rate (RR) adjusted to achieve a $Paco_2$ between 35 and 45 mm Hg. Fio_2 was kept at 1.0 during the entire experiment. During preparation, an indwelling catheter was inserted in the right internal carotid artery and a pulmonary artery catheter was advanced through a sheath, placed in the right external jugular vein for continuous monitoring of mean arterial and pulmonary artery pressure. Catheters were placed in the left femoral artery and right femoral vein (15F and 17F, respectively). After preparation, noninjured lungs were recruited with continuous airway pressure (CPAP) of 30 cm H_2O for 30 seconds, followed by 15 minutes of stabilization and baseline measurements (Baseline 1).

Experimental ARDS was induced with a double-hit consisting of saline lung lavage and injurious MV. Saline lung lavage (first hit) was performed without changing the ventilator settings until Pao_2/Fio_2 was less than 200 mm Hg for greater than or equal to 30 minutes, when measurements were performed (Injury) (13). After anticoagulation with heparin, an interventional lung assist (ILA; Novalung GmbH, Heilbronn, Germany) was connected to

the catheters in the femoral artery and vein, in order to allow extracorporeal Co_2 removal. Lungs were separated introducing a modified right-sided double-lumen tube (DLT) through a tracheotomy, with the bronchial tip placed into the left main bronchus and two separate ventilators connected to either the tracheal or bronchial lumen of the DLT.

Acquisition of Respiratory Signals, Gas Exchange, and Hemodynamics

Airflow was obtained from internal sensors of the mechanical ventilator. Airway pressure (Paw) was monitored by a pressure transducer (163PC01D48-PCB; Sensortechnics GmbH, Puchheim, Germany). Arterial and mixed venous blood samples were analyzed for respiratory gases and pH using an ABL 80 blood gas analyzer (Radiometer, Copenhagen, Denmark). Mean arterial and pulmonary artery pressures were measured continuously, whereas cardiac output (CO) was measured with the pulmonary artery catheter by means of a conventional thermodilution method.

Interventional Protocol

Time course of interventions is presented in Figure 1. Following lung separation, lungs were recruited with CPAP of 40 cm H_2O for 30 seconds. Throughout the text, the right lung is termed “control lung,” and the left lung is termed “VILI lung.”

In the control lung, CPAP was reduced to 20 cm H_2O and maintained until the end of the experiment. A similar recruitment maneuver was repeated every 30 minutes to minimize right lung atelectasis. Since the control lung was not submitted to tidal ventilation, and lung injury is likely nonhomogenous, derecruitment might occur in certain lung regions even at a relatively high airway pressure of 20 cm H_2O. We opted for the CPAP of 20 cm H_2O in order to minimize a possible shift of perfusion to the VILI lung, while avoiding lung collapse in the control lung as far as possible. In the VILI lung, a decremental PEEP trial was performed under pressure-controlled ventilation ($V_T \approx 3$ mL/kg). The PEEP trial was started at 36 cm H_2O to assure that the region of the pressure–volume curve of the respiratory system describing over distension would be achieved, and appropriately represented in pressure–volume curve of the respiratory system. PEEP was reduced by steps of 2 cm H_2O until zero, and every step was maintained for 2 minutes. Before every PEEP change, respiratory system mechanics were recorded.

Following the PEEP trial, animals were randomly assigned to two groups ($n = 5$ per group): 1) atelectrauma or 2) volutrauma, which were characterized by different PEEP settings. In volutrauma, to ensure complete lung recruitment and over-distension at end-expiration, PEEP was set one step above the level where dynamic compliance had increased by more than 5% compared with the previous value during the PEEP trial. In atelectrauma, low PEEP was adjusted at the opposite end of the pressure–volume curve to achieve a ΔP comparable with the one measured at volutrauma PEEP. Before PEEP settings were changed, the VILI lung was recruited again (CPAP of 40 cm H_2O for 30 s) in volutrauma animals. Co_2 removal was assisted extracorporeally (ILA; Novalung GmbH). RR was adjusted if $Paco_2$ rose above 80 mm Hg despite maximal sweep gas flow or fell below 50 mm Hg in case sweep gas flow needed to be maintained because of severe hypoxemia. Other MV settings were kept constant in both groups until the end of the experiments. The desired type of injurious MV

(second hit) was maintained for 4 hours. Measurements of hemodynamics, gas exchange, and respiratory variables were performed every 60 minutes during 4 hours.

At the end of the experiments, animals were killed with IV injections of thiopental (2 g) followed by KCl (1 M; 50 mL).

Respiratory Mechanics Variables

The mechanical properties of the respiratory system were calculated from 5-minute acquisitions of respiratory signals using a volume-dependent single-compartment model, as shown in Equation 1.

$$P_{aw}(t)=R_{rs}\cdot \dot{V}(t)+(E_1+E_2\cdot V(t))\cdot V(t)+P_0 \quad [1]$$

where V is volume, is airflow, t is time, and P_0 is the total airway pressure at end-expiration. R_{rs} represents the resistance of the respiratory system, and E_1 and E_2 are the volume-independent and volume-dependent components of the respiratory system elastance (E_{rs}), respectively. The distension index $\%E_2$ was computed from Equation 2.

$$\%E_2=100\times(E_2\times V(t))/(E_1+E_2\times V(t)) \quad [2]$$

Lung Imaging Protocol

Two hours after randomization, a low dose helical CT of the thorax was obtained for attenuation correction of PET images (CT-based attenuation correction [CTAC]) (Biograph16 Hirez PET/CT; Siemens, Knoxville, TN). Images were reconstructed with 2.0-mm slice thickness, yielding matrices with 512 × 512 pixels (1.37 × 1.37 mm^2). Segmentation was performed on CTAC scans to define regions of interest (ROI), from which major airways and vessels were excluded, and to compute gas fraction (F_{GAS}) from the linear relation between tissue attenuation expressed in Hounsfield units (HU) and lung density (F_{GAS} = HU/−1,000). The masks obtained from CTAC were also applied to PET images.

[^{18}F]FDG (100–216 MBq) was infused, and, starting at the beginning of [^{18}F]FDG infusion, sequential PET frames (6 × 30″, 7 × 60″, 15 × 120″, 1 × 300″, 3 × 600″) were acquired over 75 minutes, and pulmonary arterial blood was sampled (12 × 15″, 4 × 30″, 5 × 60″, 11 × 300″, 75′). Tracer plasma activity was measured in a γ counter cross-calibrated with the PET scanner. The field of view (15 cm) was set above the diaphragmatic dome to reduce artifacts due to motion of the respiratory muscles. Images were reconstructed with 2.0-mm slice thickness, yielding matrices with 168 × 168 pixels (2.03 × 2.03 mm^2). The reconstruction was carried out iteratively (ordered subset expectation maximization, six iterations, four subsets, postfiltering Gauss 5 mm) with correction for scatter and attenuation.

The [^{18}F]FDG uptake in each ROI was modeled using the Sokoloff three-compartment model adapted by Reivich et al (14), and the net uptake rate of [^{18}F]FDG (K_i) was calculated. To account for differences in lung inflation and blood volume in each ROI and different animals, K_i was normalized to lung tissue fraction (F_{TISSUE}), thus computing the specific K_i (K_{iS}) as in Equation 3.

$$K_{iS}=K_i/F_{TISSUE}=K_i/(1-F_{GAS}-F_{BLOOD}); \quad [3]$$

where F_{BLOOD} is the fractional volume of the blood compartment obtained from the Sokoloff model. Variables were extracted for each lung, and five isogravimetric subregions along the ventral-dorsal axis. Isogravimetric subregions were used to compensate for differences in lung size and ensure comparable tissue content per ROI across the gravitational gradient. For graphic illustration, [^{18}F]FDG-uptake rate was calculated according to the Patlak model (K_{iP}) and normalized to F_{TISSUE} (15).

After a single-frame PET-scan acquiring the residual background [^{18}F]FDG activity, the distribution of specific regional perfusion ($\dot{Q}_S$) was determined using a ^{68}Ga-labeled tracer and PET scanning, as previously described (16). Shortly, ^{68}Ga-labeled albumin microspheres were injected, and their distribution was acquired in three bed positions to include the whole lung. Image reconstruction was carried out iteratively (ordered subset expectation maximization, six iterations, four subsets, postfiltering Gauss 5 mm) with attenuation correction. The voxel size of the perfusion scans was 2.03 × 2.03 × 2 mm^3 yielding matrices with 168 × 168 pixels. The ^{68}Ga net activity (^{68}Ga PET$_{\mathrm{net}}$) of the attenuation-corrected images was calculated by subtraction of the background [^{18}F]FDG activity, taking into account the decay half-lives of ^{18}F and ^{68}Ga. For the whole VILI and control lungs, as well as for the five isogravimetric subregions along the ventral-dorsal axis, the ^{68}Ga PET$_{\mathrm{net}}$ inside the ROI (^{68}Ga-PET$_{\mathrm{net,ROI}}$) was normalized to total [^{68}Ga] PET$_{\mathrm{net}}$ of the whole lung (^{68}Ga-PET$_{\mathrm{net,TOTAL}}$) and multiplied by the CO ($\dot{Q}_T$) measured at the time point corresponding to the PET scan, yielding the regional perfusion, as shown in Equation 4.

$$\dot{Q}_i=\frac{^{68}\mathrm{Ga-PET}_{net,ROI}}{^{68}\mathrm{Ga-PET}_{net,TOTAL}}\times\dot{Q}_T \quad [4]$$

Aeration compartments were obtained from helical chest CT scans during end-inspiration, end-expiration, and mean lung volume hold maneuvers (17). The CT scanner was set as follows: collimation, 16 × 0.75 mm; voltage, 120 kV; and tube current-time product, 120 mAs. Images were reconstructed using 1.0-mm slice thickness, yielding matrices with 512 × 512 pixels with a size of 0.508 × 0.508 mm^2. For the whole VILI and control lungs, as well as for five isogravimetric subregions along the ventral-dorsal axis, aeration compartments at end-expiration and end-inspiration were computed based on previously described thresholds (17): ranges of −1000 to −900 HU, −900 to −500 HU, −500 to −100 HU, and −100 to +100

HU were used to define the hyperaerated, normally aerated, poorly aerated, and nonaerated compartments, respectively. Tidal recruitment was calculated as the decrease in the percentage of nonaerated compartment from end-expiration to end-inspiration. Tidal hyperaeration was calculated as the increase in the percentage of hyperaeration from end-expiration to end-inspiration (18). CT data detected at mean lung volume were used to calculate lung mass of the whole VILI and control lungs, respectively (19).

Statistics

The sample size calculation for testing the primary hypothesis ($K_{I\!S}$ is higher in volutrauma than atelectrauma in pigs) was based on effect estimates obtained from pilot studies and data from the literature (20). Accordingly, we expected a sample size of five animals to provide the appropriate power ($1 - \beta = 0.8$) to identify significant ($\alpha = 0.05$) differences in $K_{I\!S}$ between volutrauma and atelectrauma, considering an expected effect size d equal to 2.20, and Wilcoxon and Mann-Whitney tests. Data are presented as median [interquartile range], unless stated otherwise. PET and CT variables were tested with Wilcoxon and Mann-Whitney U tests with Bonferroni-Holm adjustments for multiple comparisons. Data from respiratory, hemodynamic, and gas exchange variables were analyzed as follows: comparability of groups at Baseline 1 and Injury as well as resulting V_T and ΔP after the PEEP trial was tested with an unpaired t test, and differences among groups after randomization were tested with general linear model statistics using Injury as covariate, and adjusted for repeated measurements according to the Sidak procedure. The statistical analysis was performed with SPSS version 21 (SPSS, Chicago, IL). The global significance level for all performed tests was α equal to 0.05.

RESULTS

Body weight, number of saline lung lavages, as well as cumulative doses of crystalloids and colloids did not differ between volutrauma and atelectrauma (**ESM** Table 1, Supplemental Digital Content 1, http://links.lww.com/CCM/B808). Lung lavage induced a decrease in Pao_2 and an increase in $Paco_2$, but both variables did not differ between groups. During VILI, except of a nonsignificant trend toward a higher $Paco_2$ during volutrauma, volutrauma and atelectrauma resulted in comparable gas-exchange and hemodynamics (Table 1).

V_T was comparable involutrauma and atelectrauma (Table 2). Peak and mean airway pressure, as well as the percentage of volume-dependent elastance, were higher in volutrauma, whereas elastance and resistance, as well as ΔP, were increased in atelectrauma. **ESM** Figure 1 (Supplemental Digital Content 1, http://links.lww.com/CCM/B808) shows the PEEP settings in volutrauma and atelectrauma.

Figure 2 shows the distribution of aeration as well as single-slice images of F_{GAS}, $\dot{Q}_s$, and K_{iP} normalized to $(1 - F_{GAS})$ in one representative animal of each group. Volutrauma increased $K_{I\!S}$ in the ventilated lung compared with atelectrauma and to the respective nonventilated lung (Fig. 3). In atelectrauma, $K_{I\!S}$ did not differ between VILI and control lung. As shown in Figure 4, $K_{I\!S}$ was particularly increased in mid-ventral, central, and mid-dorsal lung regions in volutrauma compared with atelectrauma, and in VILI compared with the control lung. F_{GAS} was higher, whereas F_{BLOOD} was lower, in volutrauma compared

with atelectrauma, and the respective control lung in all regions. $\dot{Q}_i$ did not differ significantly between volutrauma and atelectrauma, but was reduced in the VILI compared with the control lung in both groups. Weights of VILI and control lungs were 293.9 g [208.2–313.1 g] and 410.1 g [350.6–487.6 g] in volutrauma ($p = 0.043$), and 326.2 g [268.6–521.2 g] and 423.3 g [343.6–586.3 g] in atelectrauma ($p = 0.080$), respectively. Weights of VILI lungs did not differ between volutrauma and atelectrauma ($p = 0.251$). Hyper- and normally aerated compartments were increased, whereas the nonaerated compartment was decreased at end-inspiration and end-expiration, in volutrauma compared with atelectrauma. At end-inspiration, the poorly aerated compartment was reduced in ventral and mid-ventral lung regions in volutrauma compared with atelectrauma (Fig. 5). Volutrauma compared with atelectrauma increased tidal hyperaeration in all, except to ventral, lung regions, while decreasing tidal recruitment (Fig. 6). Further results are presented in the supplemental data (Supplemental Digital Content 1, http://links.lww.com/CCM/B808).

DISCUSSION

In the current experimental model of ARDS, we found that volutrauma, as compared with atelectrauma: 1) increased lung inflammation, mainly in mid-ventral, central, and mid-dorsal lung regions; 2) decreased F_{BLOOD} along the ventral-dorsal axis, at comparable perfusion; 3) decreased non- and poorly aerated, but increased normally and hyperaerated lung compartments; and 4) was associated with more tidal hyperaeration and less tidal recruitment.

To our knowledge, this is the first study determining the effects of volutrauma and atelectrauma at comparable low V_T and RRs on regional lung inflammation, perfusion, aeration compartments, and tidal hyperaeration as well as recruitment. We used saline lung lavage as a first hit because it has little impact on lung inflammation and, therefore, represents an ideal way to investigate the effects of ventilation strategies in VILI (21). The double-hit model of ARDS consisting of saline lung lavage followed by injurious MV reproduces typical features of ARDS in humans regarding lung function, inflammation, and damage. Using lung separation combined with extracorporeal Co_2 removal, which was necessary to avoid excessive hypercapnia with resulting severe respiratory acidosis caused by one-lung ventilation with low V_T, we isolated the individual contributions of volutrauma and atelectrauma on lung inflammation during VILI. We opted for a recruitment maneuver with sustained inflation because it is highly effective in opening lungs in a model of moderate ARDS (20, 22). In addition, after recruiting lungs and differently from clinical lung protective MV, we selected levels of PEEP according to the pressure–volume curve of the respiratory system, in order to induce predominantly volutrauma or atelectrauma. Previous studies on injurious ventilation strategies were not able to avoid overlapping effects of atelectrauma and volutrauma on lung histology (5), cytokine release (23), and also lung inflammation measured by [^{18}F]FDG uptake (24, 25).

PET with [^{18}F]FDG represents a well-established method to assess pulmonary inflammation in vivo, which has been increasingly used in a variety of pulmonary diseases (26). Normal tissue shows a relatively low rate of glucose metabolism. Thus, in absence of neoplasy,

[^{18}F]FDG accumulates in inflammatory cells, especially neutrophils, as shown by micro-autoradiography of bronchoalveolar lavage fluid in patients with pneumonia (27).

The observation that lung inflammation was higher in volutrauma than atelectrauma can be explained by several factors, including static as well as dynamic stress and strain of lung units, driving pressure, regional perfusion, and blood volume.

In volutrauma, the static component of strain was higher than in atelectrauma. Since V_T was low and comparable in both groups, the dynamic component of strain was comparatively lower in volutrauma. Furthermore, the static stress was higher in volutrauma than atelectrauma as evidenced by increased inspiratory airway pressures. Consequently, higher static stress and strain likely contributed to the increased lung inflammation in volutrauma.

Previous experimental (5, 28) and clinical (6) studies reported that activation of inflammation in dependent lung regions is lower than in nondependent ones, suggesting that the contribution of volutrauma to VILI is greater than that of atelectrauma. However, those studies focused on dynamic and not static stress and strain. In contrast to our study, other investigators reported higher regional lung inflammation in dependent compared with nondependent lung zones during injurious ventilation in sheep (25). These differences could be explained by the fact that high V_T, and consequently higher inspiratory pressures, was combined with low PEEP, possibly promoting both atelectrauma and volutrauma in dependent zones. Different from our data, recent experimental evidence suggested that the pulmonary [^{18}F]FDG uptake correlates with dynamic strain (24). This discrepancy could be explained by the fact that in our animals the relatively large static component predominated over the dynamic strain component. It is worth noting that ΔP, which is a surrogate of dynamic stress and has major influence on lung inflammation (29), increased in atelectrauma, but not in volutrauma. Thus, the difference in K_{iS} between volutrauma and atelectrauma may have been even underestimated.

Our data suggest that the pulmonary perfusion did not influence the differences in lung inflammation because $\dot{Q}_i$ did not differ between volutrauma and atelectrauma. However, the transmural pressure, that is, the difference between intracapillary and alveolar-interstitial pressure, was likely decreased in volutrauma, since the average alveolar pressure was higher in that group. Given that higher transmural pressures contribute to VILI (30, 31), the contribution of volutrauma to VILI would be even higher if this factor was comparable between groups.

Even though the pulmonary [^{18}F]FDG uptake cannot be solely ascribed to neutrophils, this radiotracer has high specificity for those cells in injured lungs (12, 32). Accordingly, the [^{18}F]FDG uptake reflects not only an increased number of neutrophils but also augmented metabolic activity. Provided that the concentration of white blood cells was comparable between groups, the finding that F_{BLOOD} was decreased in volutrauma compared with atelectrauma might indicate that higher lung inflammation was determined mainly by enhanced metabolism of neutrophils, rather than their recruitment into the lung parenchyma. However, we cannot exclude that proportionally higher neutrophil infiltration also occurred because of increased capillary endothelial damage.

Different factors contribute to lung mass, namely pulmonary edema, blood mass, lung and inflammatory cells mass, as well as connective tissue. Given that F_{BLOOD} was lower in volutrauma, we hypothesize other components of lung mass increased, including pulmonary edema and/or inflammatory cells mass. However, since lung weight in VILI lungs did not differ between volutrauma and atelectrauma, CT densities do not explain differences in lung inflammation between groups.

The distributions of aeration compartments confirmed that volutrauma was associated with hyper- and normally aerated lung regions, whereas atelectrauma resulted in non- and poorly aerated tissue along the ventral-dorsal gradient. In volutrauma, the amount of tidal hyperaeration in all isogravimetric regions was comparatively low, suggesting a more relevant role of static strain to promote pulmonary [^{18}F]FDG uptake. However, in volutrauma, the dynamic component of strain possibly played a role, since lung inflammation was increased mainly in central lung regions, that is, approximately followed the distribution of tidal hyperaeration. In atelectrauma, a similar distribution pattern of tidal recruitment and lung inflammation was observed, suggesting a higher contribution of dynamic strain to pulmonary [^{18}F]FDG uptake. In fact, the static component of strain in atelectrauma was likely negligible. However, despite the use of low V_T, we cannot completely exclude that inflammation in the atelectrauma group was determined, at least in part, by shear stress, which was likely not present in the volutrauma group. Such findings are in line with recent reports, which identified increased inflammation in ventilated compared with atelectatic lung tissue in experimental ARDS (33, 34).

Potential Implications of the Findings

Our findings provide evidence that the static component of stress and strain plays an important role in the development of VILI. This insight may be relevant not only for the understanding of the mechanisms of VILI, but also to improve protective MV. In ARDS, to fulfill its potential protective effects, a proper titrated-individualized PEEP needs be preceded by a proper titrated-individualized maximum recruitment strategy. Then, PEEP not only may decrease atelectrauma but also has the potential to reduce volutrauma (20, 22). However, the distribution of aeration might be nonhomogenous, and certain lung regions can be under higher static stress and strain. The present results suggest that volutrauma areas might be at higher risk for VILI, even if the dynamic component of stress and strain is low, but its static component is high, for example, during high PEEP. In line with this rationale, our data might contribute to understand why high-frequency oscillatory ventilation has not been found more beneficial (35) or even more harmful (36) than conventional MV in ARDS.

In our study, we isolated as far as possible the respective contributions of volutrauma and atelectrauma by achieving extreme situations in a proof-of-concept investigation. Thereby, relatively high static levels of stress/strain were obtained in the volutrauma group, which likely outweighed the contribution of the dynamic component to inflammation. As shown in an in vitro investigation (37), cellular death progressively increases at higher dynamic stress and higher RR. However, at lower RR, the contribution of static and dynamic stress/strain on cellular death is comparable. This is in line with our data, showing the relative importance of static stress/strain when dynamic stress is minimized. Therefore, a possible contribution of

our study is to draw the attention to the role of static, in addition to dynamic, pressures to determine VILI.

Limitations

The present study has several limitations. First, our data were obtained under extreme conditions of overdistension, in volutrauma, and of lung collapse, in atelectrauma. Thus, the MV settings used were designed to provide further insight into the mechanisms of VILI and did not reproduce clinical practice. Second, we used a measure of regional metabolic activity as a surrogate for the contribution of volutrauma and atelectrauma to VILI and did not assess pro-inflammatory markers. However, the pulmonary [^{18}F]FDG uptake has been validated as a reliable marker of neutrophilic inflammation in injured lungs (12, 25, 38–41). Nevertheless, in the presence of atelectasis, neutrophil accumulation may be less pronounced in injured small airways (4), and the contribution of atelectrauma to VILI may have been underestimated. Third, we also did not assess the histologic changes induced by volutrauma or atelectrauma. However, histologic methods assess neutrophil counts or sequestration and [^{18}F]FDG uptake reflects neutrophil activation, which might differ from each other (24). In fact, acute lung injury may depend more on neutrophil activation than the absolute neutrophil number (38). Fourth, we normalized the [^{18}F]FDG uptake to tissue mass, possibly introducing artifacts of density estimates by CT in the calculations of inflammation. Nonetheless, given that the field of view in PET is limited to part of the lungs only (15 cm across the cranial-caudal axis), this procedure was necessary to allow comparison between lungs with lower (volutrauma) and higher tissue density (atelectrauma). Fifth, we used static end-inspiratory and end-expiratory CT scans with breath holding to study dynamic VILI mechanisms. Breath holding may have introduced artifacts because it does not allow strictly static conditions because of instability of lung regions during the tidal ventilation pause. Theoretically, dynamic CT scans could overcome such limitation. Nonetheless, the use of dynamic CT would have led to more pronounced artifacts, especially in the atelectrauma group, because of the cranial-caudal dislocation of the lung across a relatively thin field of view. Sixth, overdistension could not be completely avoided in atelectrauma. However, tidal hyperaeration was limited to the most nondependent lung zones and may have led to an overestimation of the pulmonary [^{18}F]FDG uptake in atelectrauma group. Seventh, recruitment maneuvers were repeated every 30 minutes in the control lung to minimize collapse, which potentially increased inflammation of the control lung. Nonetheless, such maneuvers were performed in the same way in both groups, and the interpretation of the comparative contribution of volutrauma and atelectrauma to VILI was not affected.

CONCLUSIONS

In this experimental model of ARDS, volutrauma promoted higher lung inflammation than atelectrauma at comparable low V_T and lower ΔP, suggesting that static stress and strain are major determinants of VILI.

Acknowledgments

Supported by a grant of the MeDDrive Program, Medical Faculty Carl Gustav Carus, Dresden, Germany. The positron emission tomography/computed tomography device was a gift from the German Federal Ministry of Education and Research (BMBF contract 03ZIK42/OncoRay), Bonn, Germany.

We are indebted to Susanne Henninger Abreu, research nurse, and the research fellows of the Pulmonary Engineering Group, University Hospital Carl Gustav Carus, Technische Universitat Dresden, Germany, for their assistance in conducting the experiments and processing lung imaging data. We also thank Mrs. Gabriele Kotzerke and Mrs. Kathrin Gericke, technical radiology assistants from the Institute of Nuclear Medicine, University Hospital Dresden, Dresden, Germany, for their support.

References

1. Hess DR, Thompson BT, Slutsky AS. Update in acute respiratory distress syndrome and mechanical ventilation 2012. Am J Respir Crit Care Med. 2013; 188:285–292. [PubMed: 23905523]
2. Slutsky AS, Ranieri VM. Ventilator-induced lung injury. N Engl J Med. 2013; 369:2126–2136. [PubMed: 24283226]
3. Dreyfuss D, Soler P, Basset G, et al. High inflation pressure pulmonary edema. Respective effects of high airway pressure, high tidal volume, and positive end-expiratory pressure. Am Rev Respir Dis. 1988; 137:1159–1164. [PubMed: 3057957]
4. Muscedere JG, Mullen JB, Gan K, et al. Tidal ventilation at low airway pressures can augment lung injury. Am J Respir Crit Care Med. 1994; 149:1327–1334. [PubMed: 8173774]
5. Tsuchida S, Engelberts D, Peltekova V, et al. Atelectasis causes alveolar injury in nonatelectatic lung regions. Am J Respir Crit Care Med. 2006; 174:279–289. [PubMed: 16675780]
6. Bellani G, Guerra L, Musch G, et al. Lung regional metabolic activity and gas volume changes induced by tidal ventilation in patients with acute lung injury. Am J Respir Crit Care Med. 2011; 183:1193–1199. [PubMed: 21257791]
7. de Prost N, Costa EL, Wellman T, et al. Effects of surfactant depletion on regional pulmonary metabolic activity during mechanical ventilation. J Appl Physiol (1985). 2011; 111:1249–1258. [PubMed: 21799132]
8. Kawano T, Mori S, Cybulsky M, et al. Effect of granulocyte depletion in a ventilated surfactant-depleted lung. J Appl Physiol (1985). 1987; 62:27–33. [PubMed: 3558186]
9. Tsuno K, Miura K, Takeya M, et al. Histopathologic pulmonary changes from mechanical ventilation at high peak airway pressures. Am Rev Respir Dis. 1991; 143:1115–1120. [PubMed: 2024823]
10. Musch G. Positron emission tomography: A tool for better understanding of ventilator-induced and acute lung injury. Curr Opin Crit Care. 2011; 17:7–12. [PubMed: 21169828]
11. Reiss M, Roos D. Differences in oxygen metabolism of phagocytosing monocytes and neutrophils. J Clin Invest. 1978; 61:480–488. [PubMed: 202614]
12. Jones HA, Clark RJ, Rhodes CG, et al. *In vivo* measurement of neutrophil activity in experimental lung inflammation. Am J Respir Crit Care Med. 1994; 149:1635–1639. [PubMed: 7516252]
13. Lachmann B, Robertson B, Vogel J. *In vivo* lung lavage as an experimental model of the respiratory distress syndrome. Acta Anaesthesiol Scand. 1980; 24:231–236. [PubMed: 7445941]
14. Reivich M, Kuhl D, Wolf A, et al. The [18F]fluorodeoxyglucose method for the measurement of local cerebral glucose utilization in man. Circ Res. 1979; 44:127–137. [PubMed: 363301]
15. Patlak CS, Blasberg RG, Fenstermacher JD. Graphical evaluation of blood-to-brain transfer constants from multiple-time uptake data. J Cereb Blood Flow Metab. 1983; 3:1–7. [PubMed: 6822610]
16. Kotzerke J, Andreeff M, Wunderlich G, et al. Ventilation-perfusion-lungscintigraphy using PET and 68Ga-labeled radiopharmaceuticals. Nuklearmedizin. 2010; 49:203–208. [PubMed: 21057723]
17. Puybasset L, Cluzel P, Gusman P, et al. Regional distribution of gas and tissue in acute respiratory distress syndrome. I. Consequences for lung morphology. CT Scan ARDS Study Group. Intensive Care Med. 2000; 26:857–869. [PubMed: 10990099]

18. Malbouisson LM, Muller JC, Constantin JM, et al. CT Scan ARDS Study Group. Computed tomography assessment of positive end-expiratory pressure-induced alveolar recruitment in patients with acute respiratory distress syndrome. Am J Respir Crit Care Med. 2001; 163:1444–1450. [PubMed: 11371416]
19. Gattinoni L, Caironi P, Pelosi P, et al. What has computed tomography taught us about the acute respiratory distress syndrome? Am J Respir Crit Care Med. 2001; 164:1701–1711. [PubMed: 11719313]
20. Pelosi P, Gama de Abreu M, Rocco PR. New and conventional strategies for lung recruitment in acute respiratory distress syndrome. Crit Care. 2010; 14:210. [PubMed: 20236454]
21. Matute-Bello G, Frevert CW, Martin TR. Animal models of acute lung injury. Am J Physiol Lung Cell Mol Physiol. 2008; 295:L379–L399. [PubMed: 18621912]
22. Farias LL, Faffe DS, Xisto DG, et al. Positive end-expiratory pressure prevents lung mechanical stress caused by recruitment/derecruitment. J Appl Physiol (1985). 2005; 98:53–61. [PubMed: 15377644]
23. Wilson MR, Choudhury S, Goddard ME, et al. High tidal volume upregulates intrapulmonary cytokines in an in vivo mouse model of ventilator-induced lung injury. J Appl Physiol (1985). 2003; 95:1385–1393. [PubMed: 12807894]
24. Wellman TJ, Winkler T, Costa EL, et al. Effect of local tidal lung strain on inflammation in normal and lipopolysaccharide-exposed sheep*. Crit Care Med. 2014; 42:e491–e500. [PubMed: 24758890]
25. de Prost N, Costa EL, Wellman T, et al. Effects of ventilation strategy on distribution of lung inflammatory cell activity. Crit Care. 2013; 17:R175. [PubMed: 23947920]
26. Schroeder T, Melo MF, Venegas JG. Analysis of 2-[Fluorine-18]-Fluoro-2-deoxy-D-glucose uptake kinetics in PET studies of pulmonary inflammation. Acad Radiol. 2011; 18:418–423. [PubMed: 21292507]
27. Jones HA, Sriskandan S, Peters AM, et al. Dissociation of neutrophil emigration and metabolic activity in lobar pneumonia and bronchiectasis. Eur Respir J. 1997; 10:795–803. [PubMed: 9150315]
28. Wakabayashi K, Wilson MR, Tatham KC, et al. Volutrauma, but not atelectrauma, induces systemic cytokine production by lung-marginated monocytes. Crit Care Med. 2014; 42:e49–e57. [PubMed: 23963135]
29. Protti A, Andreis DT, Monti M, et al. Lung stress and strain during mechanical ventilation: Any difference between statics and dynamics? Crit Care Med. 2013; 41:1046–1055. [PubMed: 23385096]
30. Broccard AF, Hotchkiss JR, Kuwayama N, et al. Consequences of vascular flow on lung injury induced by mechanical ventilation. Am J Respir Crit Care Med. 1998; 157:1935–1942. [PubMed: 9620930]
31. Hotchkiss JR Jr, Blanch L, Murias G, et al. Effects of decreased respiratory frequency on ventilator-induced lung injury. Am J Respir Crit Care Med. 2000; 161:463–468. [PubMed: 10673186]
32. Jones HA, Schofield JB, Krausz T, et al. Pulmonary fibrosis correlates with duration of tissue neutrophil activation. Am J Respir Crit Care Med. 1998; 158:620–628. [PubMed: 9700143]
33. Borges JB, Costa EL, Suarez-Sipmann F, et al. Early inflammation mainly affects normally and poorly aerated lung in experimental ventilator-induced lung injury*. Crit Care Med. 2014; 42:e279–e287. [PubMed: 24448197]
34. Borges JB, Costa EL, Bergquist M, et al. Lung inflammation persists after 27 hours of protective Acute Respiratory Distress Syndrome Network Strategy and is concentrated in the nondependent lung. Crit Care Med. 2015; 43:e123–e132. [PubMed: 25746507]
35. Young D, Lamb SE, Shah S, et al. OSCAR Study Group. High-frequency oscillation for acute respiratory distress syndrome. N Engl J Med. 2013; 368:806–813. [PubMed: 23339638]
36. Ferguson ND, Cook DJ, Guyatt GH, et al. OSCILLATE Trial Investigators; Canadian Critical Care Trials Group. High-frequency oscillation in early acute respiratory distress syndrome. N Engl J Med. 2013; 368:795–805. [PubMed: 23339639]

37. Tschumperlin DJ, Oswari J, Margulies AS. Deformation-induced injury of alveolar epithelial cells. Effect of frequency, duration, and amplitude. Am J Respir Crit Care Med. 2000; 162:357–362. [PubMed: 10934053]

38. Hartwig W, Carter EA, Jimenez RE, et al. Neutrophil metabolic activity but not neutrophil sequestration reflects the development of pancreatitis-associated lung injury. Crit Care Med. 2002; 30:2075–2082. [PubMed: 12352044]

39. Musch G, Venegas JG, Bellani G, et al. Regional gas exchange and cellular metabolic activity in ventilator-induced lung injury. Anesthesiology. 2007; 106:723–735. [PubMed: 17413910]

40. Costa EL, Musch G, Winkler T, et al. Mild endotoxemia during mechanical ventilation produces spatially heterogeneous pulmonary neutrophilic inflammation in sheep. Anesthesiology. 2010; 112:658–669. [PubMed: 20179503]

41. Saha D, Takahashi K, de Prost N, et al. Micro-autoradiographic assessment of cell types contributing to 2-deoxy-2-[(18)F]fluoro-D-glucose uptake during ventilator-induced and endotoxemic lung injury. Mol Imaging Biol. 2013; 15:19–27. [PubMed: 22752654]

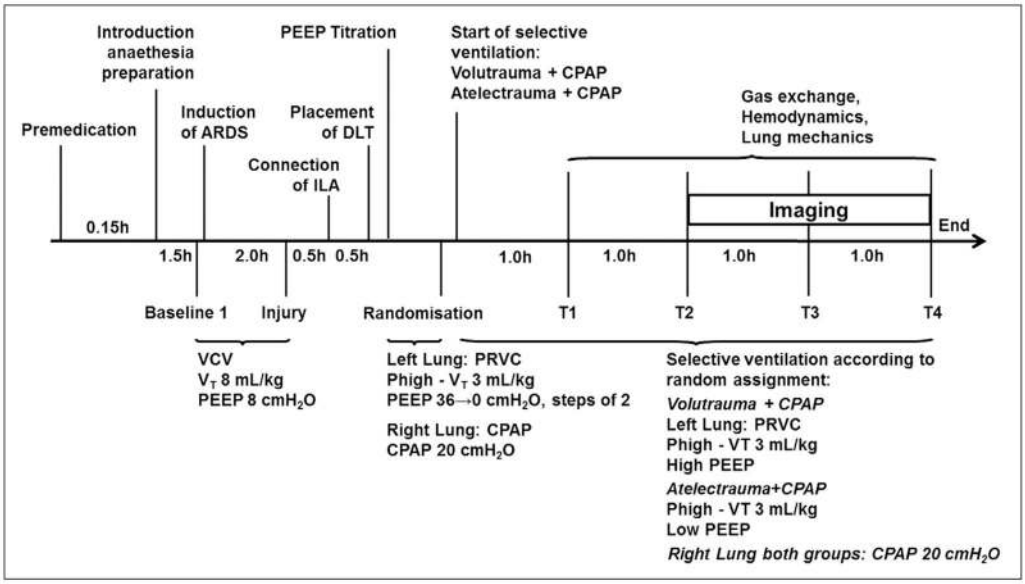

Figure 1.

Time course of interventions. ARDS = acute respiratory distress syndrome, CPAP = continuous positive airway pressure, DLT = double-lumen endotracheal tube, ILA = interventional lung assist, PEEP = positive end-expiratory pressure, PRVC = pressure-regulated volume-controlled ventilation, VCV = volume-controlled ventilation, V_T = tidal volume.

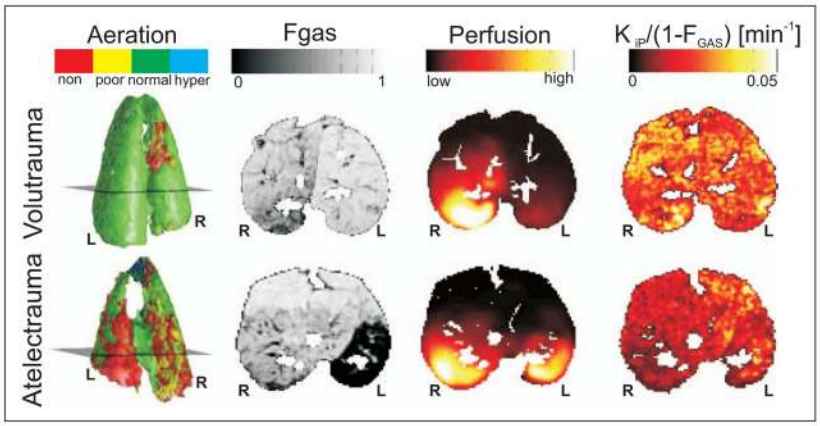

Figure 2.

Three-dimensional illustration of the distributions of aeration and single-slice images of gas fraction, perfusion, and [^{18}F]-fluorodeoxyglucose uptake rate (K_i) of representative animals. Three-dimensional illustration of the distribution of aeration, as well as 2D slice images of the gas fraction (F_{GAS}), perfusion, and [^{18}F]-fluorodeoxyglucose uptake rate ($K_{i\,P}$, computed voxel by voxel using Patlak method, and normalized to [1 – F_{GAS}]) in representative animals of the volutrauma (*upper*) and atelectrauma groups (*lower*), respectively. Two-dimensional slice images represent the maximal cross-sectional areas of the respective slice in the whole lung images. *Horizontal color bars* denote the respective scales. Hyper = hyperaerated compartment, L = left VILI (ventilated) lung, non = nonaerated compartment, normal = normally aerated compartment, poor = poorly aerated compartment, R = right control (nonventilated) lung.

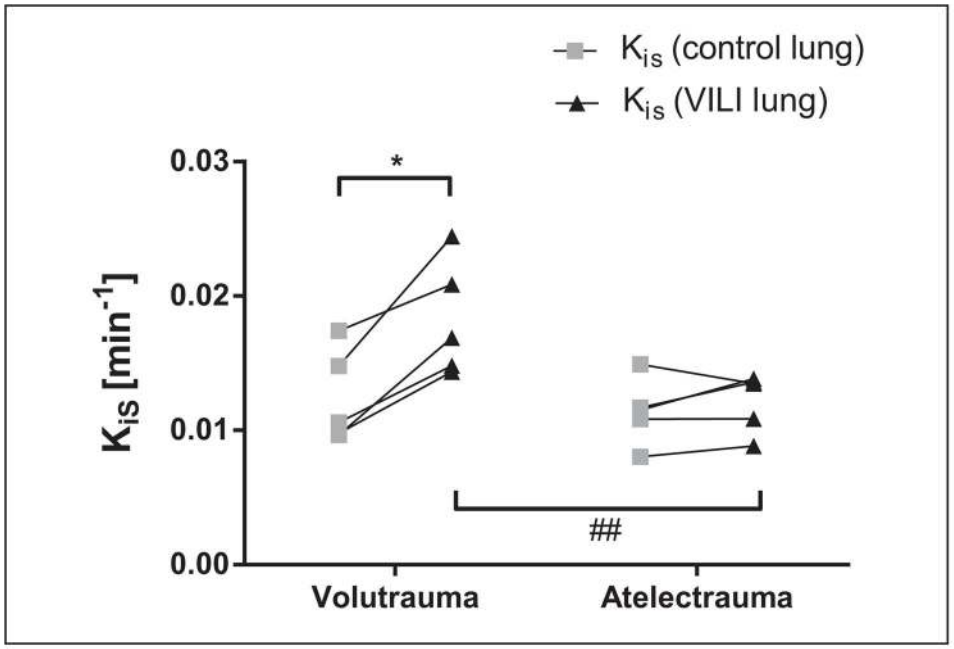

Figure 3.

[^{18}F]-fluorodeoxyglucose uptake rate (K_i) of the ventilator-induced lung injury (VILI) and control lung grouped by injury model. Specific K_i (K_{iS}) of the VILI lung (*black triangles*, ventilated lung) and corresponding control lung (*gray squares*, nonventilated lung) of all animals of the volutrauma group (*left*) and atelectrauma group (*right*). *$p < 0.05$ (vs nonventilated control lung, same injury model). #$p < 0.05$ (vs ventilated VILI atelectrauma lung). ##$p < 0.01$ (vs ventilated VILI atelectrauma lung).

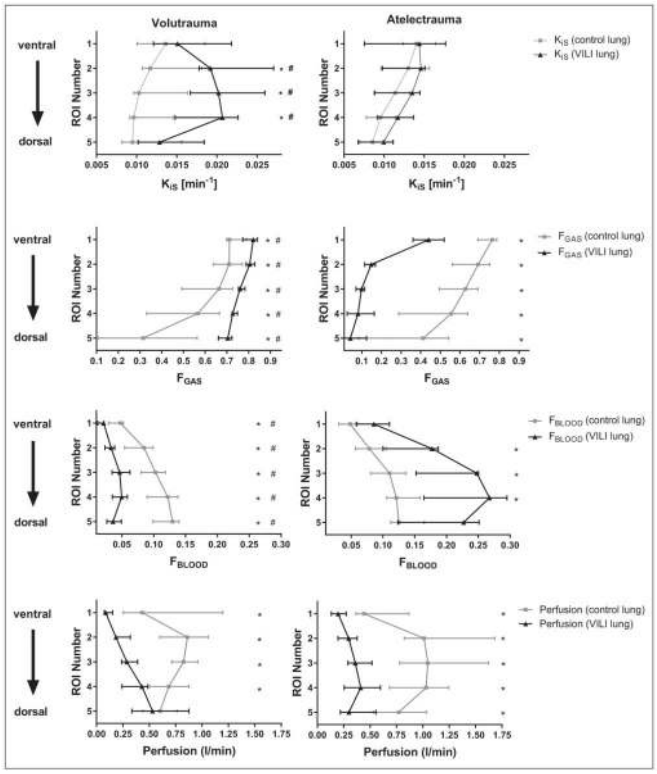

Figure 4.

Regional specific [^{18}F]-fluorodeoxyglucose net uptake rate (K_{IS}), gas fraction (F_{GAS}), blood fraction (F_{BLOOD}), and perfusion grouped by injury model. Median and interquartile range of the K_{IS}, F_{GAS}, F_{BLOOD}, and perfusion in five adjacent regions of the same lung mass reaching from ventral (regions of interest [ROI] 1) to dorsal (ROI 5) for the ventilator-induced lung injury (VILI) (*black triangles*, ventilated lung) and control lung (*gray squares*, nonventilated lung) of all animals of the volutrauma (*left*) and atelectrauma groups (*right*). *$p < 0.05$ (vs nonventilated control lung in same ROI, same injury model), #$p < 0.05$ (vs ventilated VILI atelectrauma lung in same ROI).

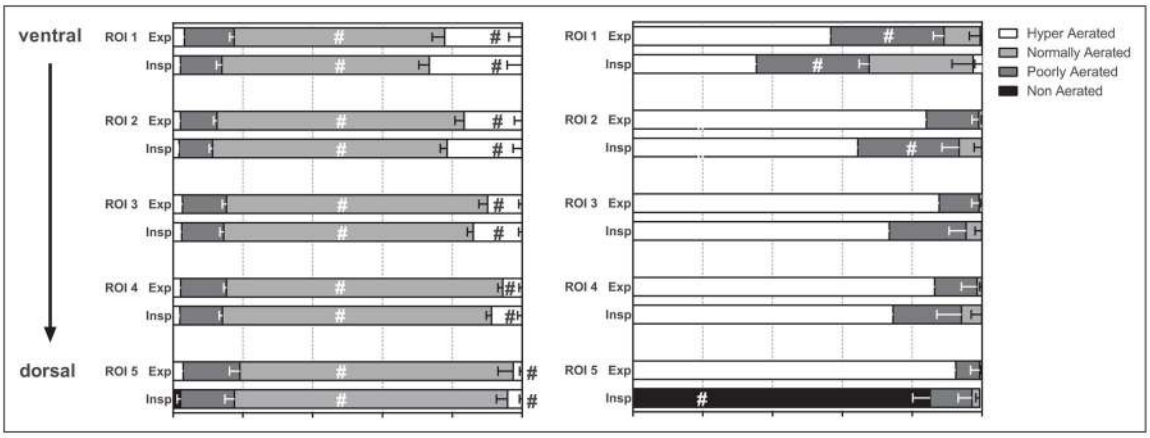

Figure 5.

Regional distribution of aeration compartments at end-inspiration and end-expiration grouped by injury model. Mean and SE of the distributions of hyperaerated (*white*), normally aerated (*dark gray*), poorly aerated (*light gray*), and nonaerated compartments (*black*) of ventilated ventilator-induced lung injury lungs in volutrauma (*left*) and atelectrauma groups (*right*), respectively, for five adjacent regions of the same lung mass reaching from ventral (regions of interest [ROI] 1) to dorsal (ROI 5) at end-expiration and end-inspiration, expressed as percent mass (%mass). #$p < 0.05$ (atelectrauma vs volutrauma for same aeration compartment in same ROI at the same lung volume). No significant difference of aeration compartments between ROIs at the same lung volume within groups.

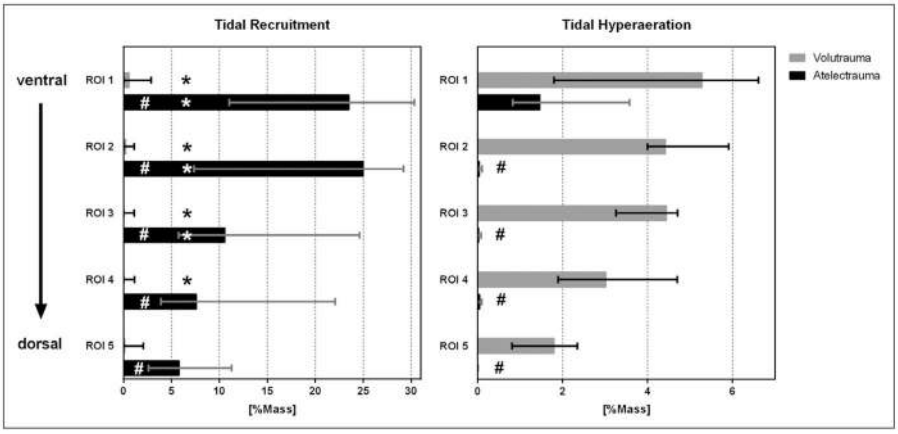

Figure 6.

Regional distribution of tidal recruitment and tidal hyperaeration. Median and interquartile range of the amount of tidal recruitment (*left*) and tidal hyperaeration (*right*) of ventilated ventilator-induced lung injury lungs in volutrauma (*gray*) and atelectrauma (*black*) groups, respectively, in five adjacent regions of the same lung mass reaching from ventral (regions of interest [ROI] 1) to dorsal (ROI 5). Tidal recruitment was calculated as the decrease in the percentage of mass of nonaerated compartment from end-expiration to end-inspiration. Tidal hyperaeration was calculated as the increase in the percentage of mass of hyperaeration from end-expiration to end-inspiration. Note different axis scales between panels. $*p < 0.05$ (tidal recruitment vs tidal hyperaeration in same ROI and injury model), $\#p < 0.05$ (atelectrauma vs volutrauma for tidal recruitment or tidal hyperaeration, respectively, in same ROI).

TABLE 1

Gas Exchange and Hemodynamics in Volutrauma in Atelectrauma Groups

Variable	Group	baseline 1	Injury	Time 1	Time 2	Time 3	Time 4	Group Effect, *p*	Time × Group Effect, *p*
Pao_2 (mm Hg)	Volutrauma	543.4±30.5	104.8±20.9	203.0±111.3	170.2±78.5	145.6±57.1	192.4±84.8	0.360	0.218
	Atelectrauma	556.8±52.7	107.8±33.1	106.0±100.1	130.0±113.8	132.8±99.1	124.4±73.6		
	p	*0.868*	*0.869*						
$Paco_2$ (mm Hg)	Volutrauma	45.2±3.7	62.6±3.0	70.0±10.4	78.2±14.2	89.2±25.1	79.8±14.3	0.073	0.504
	Atelectrauma	40.4±4.3	67.8±15.9	57.4±10.2	59.8±12.5	62.6±10.3	62.2±10.7		
	p	*0.493*	*0.501*						
pHa	Volutrauma	7.42±0.03	7.28±0.04	7.26±0.02	7.22±0.08	7.17±0.10	7.20±0.10	0.102	0.580
	Atelectrauma	7.46±0.03	7.26±0.09	7.34±0.07	7.33±0.11	7.31±0.12	7.32±0.12		
	p	0.603	0.601						
Cardiac output (L/min)	Volutrauma	4.3±1.2	4.8±1.3	5.9±0.6	6.1±0.8	5.6±0.6	5.2±0.8	0.080	0.759
	Atelectrauma	3.3±1.0	4.6±1.2	7.4±0.8	7.1±1.2	6.7±1.4	6.4±2.1		
	p	0.839	0.839						
Mean arterial pressure (mm Hg)	Volutrauma	93±18	90±12	91±11	82±31	85±14	81±12	0.731	0.922
	Atelectrauma	92±17	82±9	88±9	88±8	86±8	82±12		
	p	0.315	0.317						
Mean pulmonary arterial pressure (mmHg)	Volutrauma	26±6	34±2	43±5	44±3	44±5	44±6	0.778	0.111
	Atelectrauma	26±5	35±6	39±8	41±7	47±5	44±5		
	p	0.885	0.888						
Sweep gas flow (L/min)	Volutrauma	NA	NA	9.0±4.0	9.0±3.5	12.0±6.0	13.0±5.5	0.310	0.529
	Atelectrauma	NA	NA	6.0±4.0	8.0±6.0	8.0±6.5	8.5±6.0		

NA = not applicable.

Values are shown as mean and SD and were obtained from 10 animals in total ($n = 5$ per group). There were no missing values. Statistical significance was accepted at $p < 0.05$. Comparability of groups at Injury and Baseline 1 was tested using nonpaired *t* test with *p* values given in italics below the respective columns. Differences among groups were tested with general linear model statistics using values at the time point Injury as covariate, except of sweep gas flow, where no covariate was used. Results are shown in columns group effect and time × group effect.

Crit Care Med. Author manuscript; available in PMC 2017 September 01.

TABLE 2

Respiratory Variables in Volutrauma in Atelectrauma Groups

Variable	Group	baseline 1	Injury	Time 1	Time 2	Time 3	Time 4	Group Effect, *p*	Time × Group Effect, *p*
Minute ventilation (L/min)	Volutrauma	5.4±0.8	5.3±0.8	3.9±0.4	3.9±0.5	4.1±0.6	4.1±0.6	0.203	0.608
	Atelectrauma	4.7±0.4	4.7±0.4	3.3±0.8	3.2±0.8	3.2±0.7	3.1±0.8		
	p	0.167	0.177						
Tidal volume (mL/kg bodyweight)	Volutrauma	8.1±0.3	8.0±0.2	3.2±0.4	3.2±0.4	3.2±0.3	3.2±0.3	0.335	0.770
	Atelectrauma	8.3±0.2	8.2±0.1	3.2±0.1	3.3±0.1	3.2±0.1	3.3±0.1		
	p	0.115	0.138						
Respiratory rate (breaths/min)	Volutrauma	16.2±1.6	16.2±1.6	28.6±2.2	29.0±2.6	30.0±1.4	30.0±1.4	*0.401*	*0.156*
	Atelectrauma	15.0±0.0	15.0±0.0	28.6±1.9	26.8±3.0	26.4±4.3	26.0±4.2		
	p	0.141	0.178						
Peak airway pressure (cm H_2O)	Volutrauma	20.5±1.3	27.1±2.9	54.6±4.1	54.0±4.0	52.9±3.5	52.2±3.5	< 0.001	0.001
	Atelectrauma	21.3±2.0	29.0±4.3	32.2±7.3	33.7±7.1	34.4±6.1	34.9±6.1		
	p	0.445	0.448						
Mean airway pressure (cm H_2O)	Volutrauma	12.3±0.5	15.0±1.0	42.9±2.5	42.6±2.6	41.9±2.1	41.5±2.1	< 0.001	0.004
	Atelectrauma	12.6±1.0	15.6±1.7	15.3±4.3	16.7±4.6	17.1±4.2	17.4±4.1		
	p	0.478	0.483						
Positive end- expiratory pressure (cm H_2O)	Volutrauma	8.0±0.0	8.0±0.0	32.4±2.2	32.4±2.2	32.0±2.0	32.0±2.0	< 0.001	0.219
	Atelectrauma	8.0±0.0	8.0±0.0	0.8±1.1	1.8±2.0	1.8±1.8	1.8±1.8		
	p	1.000	1.000						
Driving pressure (cm H_2O)	Volutrauma	8.6±2.3	17.2±3.4	19.0±4.5	18.6±4.3	18.4±4.0	17.6±3.8	0.003	0.003
	Atelectrauma	10.0±3.0	19.0±6.1	26.8±5.3	28.2±5.4	29.4±4.9	30.2±4.2		
	p	0.433	0.291						
Respiratory system resistance (cm H_2O/L/s)	Volutrauma	6.2±0.2	6.6±0.6	5.2±0.8	5.2±0.6	5.4±0.6	5.4±0.8	0.003	0.410
	Atelectrauma	7.0±0.4	7.1±1.1	10.4±4.2	10.3±5.5	11.7±5.5	12.6±3.5		
	p	0.370	0.378						

Variable	Group	baseline 1	Injury	Time 1	Time 2	Time 3	Time 4	Group Effect, *p*	Time × Group Effect, *p*
Respiratory system elastance (cm H_2O/L)	Volutrauma	26.5±5.8	49.0±12.3	152.4±26.4	148.6±25.9	144.0±23.1	139.1±23.4	< 0.001	0.001
	Atelectrauma	29.4±2.8	55.1±8.4	237.8±49.7	242.8±51.1	255.9±40.3	261.7±36.3		
	p	0.381	0.385						
Percentage E2 (%)	Volutrauma	5.7±7.5	44.0±5.0	39.1±3.4	38.7±3.1	37.0±4.5	37.4±3.7	0.003	0.086
	Atelectrauma	7.9±8.2	38.6±10.1	21.2±15.9	18.5±16.6	13.5±8.1	2.3±8.7		
	p	0.313	0.324						

Driving pressure is the differences of plateau airway pressure and positive end-expiratory pressure, and percentage E2 is the volume-dependent component of the respiratory system elastance (distension index). Values are shown as mean and SD and were obtained from 10 animals in total ($n = 5$ per group). There were no missing values. Statistical significance was accepted at $p < 0.05$. Comparability of groups at Injury and Baseline 1 was tested using nonpaired *t* test with *p* values given in italics below the respective columns. Differences among groups were tested with general linear model statistics using values at the time point Injury as covariate. Results are shown in column group effect and time × group effect.